ICES J. mar. Sci., 48: 343–361. 1991

Comparative studies of coastal pelagic fish reproductive habitats: the anchovy (*Engraulis anchoita*) of the southwestern Atlantic

Andrew Bakun and Richard H. Parrish

Bakun, A., and Parrish, R. H. 1991. Comparative studies of coastal pelagic fish reproductive habitats: the anchovy (*Engraulis anchoita*) of the southwestern Atlantic. – ICES J. mar. Sci., 48: 343–361.

A framework of comparative climatology of reproductive habitats of coastal pelagic fishes is extended to the anchovy inhabiting the shelf-sea ecosystem off Argentina, Uruguay, and southern Brazil. Maritime weather reports are summarized to yield distributions of wind stress, cloud cover, insolation, sea-surface temperature, wind mixing index, and Ekman transport. These distributions are considered together with other known aspects of the oceanography of the region and with seasonal and geographical aspects of reproductive activity. Over its extensive range, *Engraulis anchoita* spawns successfully within three different configurations of environmental processes affecting transport, water column stability, and trophic enrichment. One of these, incorporating a coastal indentation downstream from a coastal upwelling center, is very similar to the most common configuration characterizing spawning grounds of eastern ocean anchovy populations. The second, featuring interleaving water masses and upwelling at the continental shelf break, exhibits similarities to the reproductive habitat of the South African anchovy. The third, involving tidal mixing fronts, has been previously noted primarily in connection with herring of higher-latitude, shallow shelf-sea systems. The study adds support to the idea that similar fish populations in different regions must solve similar basic environmental problems and that various experiences of environmental effects in different populations, when viewed from a properly posed conceptual framework, can add up to a useful accumulation of insight.

Andrew Bakun and Richard H. Parrish: Pacific Fisheries Environmental Group, Southwest Fisheries Science Center, National Marine Fisheries Service, NOAA, P.O. Box 831, Monterey, California 93942, USA.

Introduction

The population of *Engraulis anchoita*, a representative temperate zone anchovy species, extends along the Atlantic coast of South America from southern Brazil to southern Argentina. No biomass estimates are available for the entire population; however, according to Sánchez (1989) the biomass in the region off Argentina varied between 4.0 and 6.2 million metric tonnes in eight surveys made during 1967–1983. *Engraulis anchoita* is presently lightly exploited, with about 25 000 t being taken annually. It is an extremely important component of the regional ecosystem, being a major food source for a variety of predators. Hake (*Merluccius* spp.) alone, for example, may consume one million tonnes per year.[1]

Anchovies of the genus *Engraulis* comprise an extremely important component of the fishery production of the world. The Peruvian anchoveta (*Engraulis ringens*) prior to its collapse was by far the largest single fishery stock on record, reaching a peak annual production of 12 million tonnes in 1970 and by itself accounting for some one-sixth of the world's total fishery production over the period 1963–1972. Landings of the European anchovy (*Engraulis encrasicolus*) have reached 0.8 million tonnes (1984). The population of South African anchovy (*Engraulis capensis*) supported rather stable catches of 0.2 to 0.3 million tonnes for a number of years; recently the catches have increased dramatically to approach a million tonnes in 1987 (FAO, 1990). Annual catches of northern anchovy (*Engraulis mordax*) in the northeastern Pacific Ocean off the western USA and northern Mexico have been as high as 0.4 million tonnes (1981). In the northwestern Pacific, annual catches of Japanese anchovy (*Engraulis japonica*) have recently declined somewhat from a 1965 level of nearly 0.5 million tonnes. Clupeoid fishes such as anchovies and sardines are relatively short-lived, highly productive organisms which feed low in the trophic pyramid, often directly on phytoplankton. As well as being commercially important in themselves, they constitute an extremely important food base for other valuable fish species.

[1]Lasta, C. (Verbal presentation) IOC-FAO Sardine/Anchovy Recruitment Project (SARP) Consultation, La Jolla, California, 5–9 November, 1984.

1054–3139/91/030343 + 19 $03.00/0

In this paper, we examine the habitat climatology of *Engraulis anchoita* (which we call by its local name "anchoita"). The purpose is to continue to build a basis for application of the comparative method (Mayr, 1982) to the problem of identifying the physical–biological linkages controlling the population dynamics of coastal pelagic fishes. The primary environmental data source, the archived files of surface marine weather reports, is the same as used in our previous studies (e.g. Parrish *et al.*, 1981; Bakun and Parrish, 1982; Parrish *et al.*, 1983; Bakun, 1985; Bakun and Parrish, 1990). These data are available at varying densities for all regions of the oceans of the world. Thus, they represent an opportune resource for incorporating a great variety of species, habitats, and regions within a global comparative context.

In previous studies of seasonality and geography of anchovy and sardine spawning activity in eastern ocean upwelling ecosystems (Parrish *et al.*, 1981; Bakun and Parrish, 1982; Parrish *et al.*, 1983; Bakun, 1985; Roy *et al.*, 1989), a general pattern has begun to emerge. In addition to the trophic enrichment associated with the upwelling process, seasons and/or locations promoting retention of larvae near the coast while minimizing turbulent mixing of the water column appear to be favored. Temperature itself, while setting limits on geographical extents of species distributions, appears to be less important in defining favorable spawning conditions within these limits. Observational and experimental foundation for this view has been provided by the distinguished work of Reuben Lasker and his co-workers at the NOAA-NMFS Southwest Fisheries Science Center (e.g. Lasker, 1975, 1978, 1988). Several recent time series modeling studies (Mendelssohn and Mendo, 1987; Peterman and Bradford, 1987; Cury and Roy, 1989), addressing inter-year variability in reproductive success, have tended to confirm the pattern.

Western ocean boundary regions are dynamically quite different from the regions along eastern ocean boundaries. For example, there are particularly strong influences of advected momentum and generally more intense horizontal gradients in temperature and other properties. However, Bakun and Parrish (1990) found a nearly identical configuration of mechanisms, although operating over a different temperature range, appearing to determine favorable reproductive habitat for both the Brazilian sardine (*Sardinella braziliensis* = *Sardinella aurita*) population spawning in a tropical western ocean boundary ecosystem off Southeastern Brazil and the Pacific sardine (*Sardinops sagax*) population spawning in a temperate eastern ocean boundary ecosystem off Southern California. This supports the idea that populations of small coastal pelagic fishes, whatever the specifics of their environmental setting, have generally similar basic requirements that must be met for them to gain a dominant position within the regional trophic pyramid.

The Brazilian sardine can be viewed as being primarily associated with a wind-driven coastal upwelling system, which is similar in many ways to coastal upwelling systems located along eastern ocean boundaries. In contrast, the bulk of the anchoita habitat is not influenced substantially by coastal upwelling; in fact, the opposite situation of onshore surface drift and resulting coastal downwelling is dominant. In this paper, we investigate the proposition that the basic requirements for a favorable reproductive habitat may nonetheless be very similar to those in upwelling regions, and in addition may be met in a rearranged configuration of the same set of dominant environmental processes. If so, the anchoita might be justifiably incorporated in a common comparative "framework", with respect to environmental dependencies, with many of the other major pelagic-spawning clupeoid fish populations of the world's coastal marine ecosystems.

In our opinion, the case for attempting to assemble such a framework is substantial. The "fishery-environment" problems appears to be one of moderate complexity, at the least. Some framework, even a hypothetical one, is needed to organize and array whatever events and experiences of fishery-environmental interactions may be available so that, rather than remaining a collection of isolated facts and anecdotes, they can support a useful accumulation of insight. Our approach in this is diagnostic, and we do not intend to imply rigorous hypothesis testing in pointing out the patterns of correspondence that we find. However, we hope that indicating mechanistically reasonable and pervasive patterns of association among important ecological processes might support the emergence of intellectually attractive, well-focused (but not fatally oversimplified) hypotheses that could motivate the kind of observational programs, survey designs, etc., that could support rigorous tests. One should note that hypotheses formulated in this manner, being diagnosed from characteristic seasonal and geographical adaptations and behaviors rather than depending in any way on time-series results, may be regarded as *a priori* hypotheses with respect to time-series analysis. That is, they may be a guide to the selection of variables for empirical tests in a way that does not deplete, by the selection process, the minimal degrees of freedom contained in available inter-year data series (Bakun, 1985).

Anchoita reproductive habitat climatology

Adult *E. anchoita* are abundant over an extensive region (22°–47°S), from north of Cabo Frio, Brazil (Matsuura *et al.*, 1985) to just north of Cabo Tres Puntas (Ciechomski and Sánchez, 1986). Eggs and larvae occur mainly over the continental shelf which is quite broad over much of the region, and they occur, at some time of the year, over essentially the same range of latitude as do the adults. The

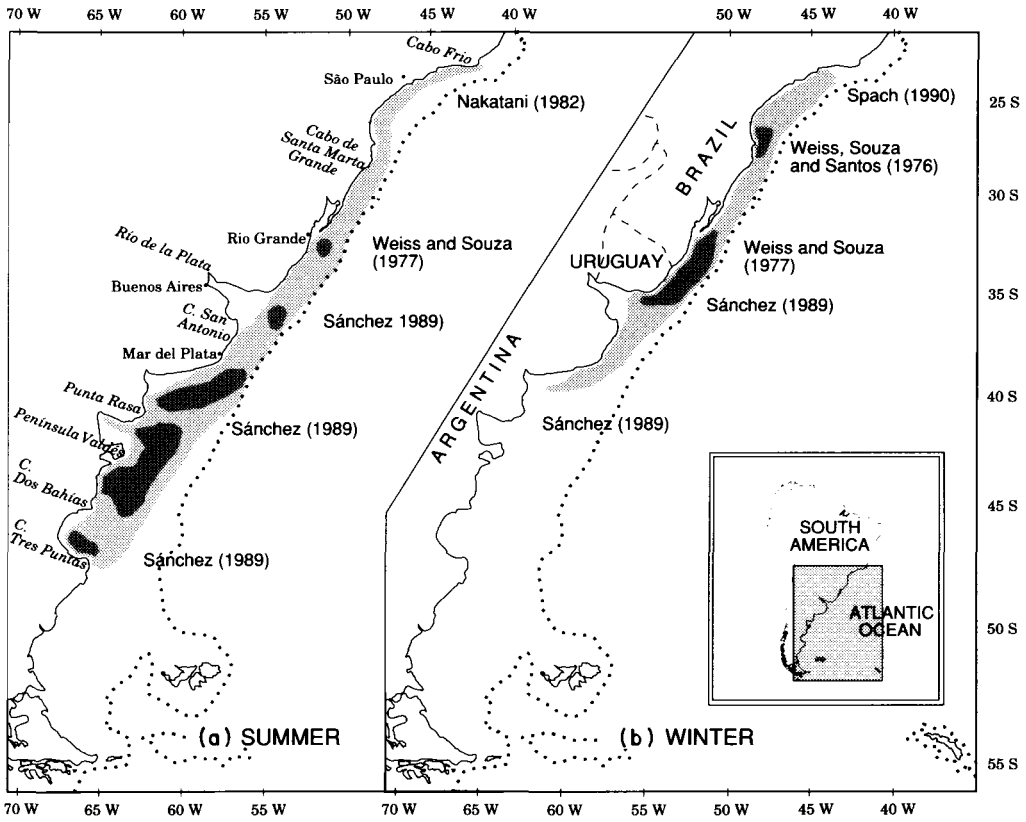

Figure 1. Coastwise extent of anchoita spawning. Light shading indicates range over which incidence of anchoita eggs has been observed. Darker shading indicates reports of substantial concentrations of eggs. (*Note that information is limited, particularly in the northern areas, and that therefore areas showing absence of concentrations may be questionable.*) References for the various features depicted are printed to the right of the areas to which they apply. The dotted line indicates the continental shelf limit (200 m isobath). (a) austral summer; (b) austral winter.

available information on the seasonal distribution of anchoita spawning has recently been reviewed (Castello, 1989; Mantero, 1989; Sánchez, 1989). Information is available for both seasonal and geographical distribution of spawning for the region off Argentina, where a large number of extensive egg and larvae surveys have been carried out. Information for the region off Uruguay and Brazil is based on a more limited number of surveys; data for the austral fall and winter are particularly sparse in the region between Cabo Frio (22°S) and Cabo de Santa Marta Grande (29°S), and no data are available for the austral summer for most of the region between Cabo de Santa Marta Grande (29°S) and Uruguay (34°S). Conclusions concerning the relative amount of spawning in the region between 22°S and 31°S must be considered preliminary as no part of the region has been surveyed twice in any of the four seasons.

During austral winter, the geographical distribution of spawning is at a minimum (Fig. 1); however, eggs and larvae are abundant off Brazil as far north as 23°S (Spach, 1990), considerable spawning occurs between 26° and 34°S (Weiss *et al.*, 1976; Weiss and Feijo de Souza, 1977), and eggs and larvae occur as far south as 40°S (Sánchez, 1989).

In spring, eggs and larvae are abundant as far north at 23°S (Nakatani, 1982; Hubold, 1982; G. Weiss, unpublished data),[2] they are at peak concentrations from 29°S to 41°S (Hubold, 1982; Sánchez, 1989; G. Weiss, unpublished data),[2] and spawning extends to about 44°S (Sánchez, 1989). Analysis of the reproductive cycle of the adults also demonstrates that reproduction peaks during the spring in northern Argentina (Brodsky and Cousseau, 1979).

The geographical extent of spawning is at a maximum during summer (Fig. 1). While still at significant levels in the region from Cabo Frio, Brazil (23°S) to Mar del Plata, Argentina (40°S), summer egg and larval concentrations are reduced from those which occur in the spring (Campaner and Honda, 1987; Weiss and Feijo de Souza, 1977; Sánchez, 1989). Eggs and larvae are at maximum concentrations between 41°S and 47°S during the summer (Sánchez, 1989).

Spawning is greatly reduced during the fall; however, eggs and larvae occur near the shelf break off São Paulo (23–27°S) in May (Nakatani, 1982; Campaner and Honda, 1987), in the vicinity of Rio Grande (29–34°S) in April (Hubold, 1982; G. Weiss, unpublished data),[2] and at relatively high concentrations off Uruguay and northern Argentina (34–38°S) throughout the fall (Sánchez, 1989).

In producing the seasonal distributions of environmental processes (Figs 2–5, 7) displayed in this section, we use the methods and procedures established in the companion paper (Bakun and Parrish, 1990; hereafter referred to as BP). Briefly, quantities of interest are estimated from individual maritime reports contained in the US National Climatic Center's file of marine surface observations (Tape Data Family – 11) and averaged by one-degree latitude/longitude quadrangles and by two-month segments of the calendar year. The vector quantities, wind stress, and Ekman transport were averaged by component (vector averaged). For reference to the formulations of the various types of estimates, and to the procedures followed in editing, smoothing of undersampled distributions, contouring, etc., we have included an adaptation of the "Methods" section from BP as an "Appendix" section to this paper.

The northern boundary of the mapped data displays (Figs 2–5, 7) overlaps the displays presented by BP. For the present study of the anchoita, there is no real need to extend the displays south of Cabo Tres Puntas (~47°S). However, the region further to the south is characterized by a very wide continental shelf and very important fishery resources, including hake, squid, pollock, etc. Because the distributions may be useful to other workers and studies, we have included the entire region as far south as the southeastern extremity of the South American Continent (Cabo San Diego) in the displays, even though the area south of 47°S latitude is not treated in the discussions of anchoita. Also, from time to time it will be useful to extend discussion northward beyond the northern limit of the data displays presented herein. In those instances, we will refer to the corresponding adjacent displays presented by BP.

Wind stress

The region lies largely within the latitude band of global-scale westerly winds. During the winter (Fig. 2a), the offshore area (i.e. the portion of the region more than about 500 km offshore) is marked by very strong westerly (eastward) stress exerted by the wind on the sea surface. A high degree of variability is indicated by the rather chaotic patterns of the vector symbols, which represent *unsmoothed independent summaries of the available* reports by one-degree latitude/longitude areal segments (thus differences between adjacent vector symbols in these distributions should not be regarded as meaningful small-scale detail, but rather as "sampling noise" due to data sparsity and consequent undersampling of a highly variable process). Also apparent at distances of several hundred kilometers from the coast is a tendency for anticlockwise veering and shearing of the vector field, implying predominance of anticyclonic wind stress curl in an offshore band parallel to the coastline trend.

With respect to this large-scale zonal flow, the area near the coast tends to lie in the "wind shadow" of the South American Continent. However, except to the north of Cabo San Antonio (~34°S), it remains a substantial fraction of one dyne cm^{-2} (0.1 Pa) during the winter season, even at near-coastal locations.

During summer (Fig. 2b), the magnitude of the wind stress is reduced substantially. The region of strong coherent westerly stress in the offshore region, which extended north of 30°S latitude in the winter, has receded south of 35°S. A region of particularly strong stress during the summer lies to the west and northwest of the Falkland (Malvinas) Islands; evidence of this feature is corroborated in the independently derived distributions for other two-month seasonal segments (not displayed for wind stress in this paper but displayed for the related turbulent mixing index and Ekman transport distributions in Figures 5 and 7). Very low average wind stress near the coast extends southward all the way to the vicinity of Cabo Dos Bahias (~45°S) during the summer.

Solar radiation and cloud cover

During the austral winter, the average portion of sky obscured by cloud cover (Fig. 3a) varies from about 50% to 55% in the extreme northern portion of the region to about 75% in the vicinity of the Falkand (Malvinas) Islands. Several local submaxima and subminima in cloud cover punctuate the larger scale north–south regional trend. For example, a strong local maximum corresponds to a region of particularly intense winds (Fig. 2a) near the seaward edge of the gridded area from ~40°S to ~46°S latitude.

The distribution of solar radiation penetrating the sea surface during winter (Fig. 3b) shows little effect of the details of the cloud cover pattern, being predominantly controlled by the very strong latitudinal gradient in day length and solar altitude which exists during the winter season. The effect of cloud cover is seen in minor features such as the northward bowing of the 20 watt m^{-2} isopleth over the Falklands.

During the summer, the cloud cover (Fig. 3c) is ~55% in the extreme northern portion of the region and ~70% near 55°S latitude. There is a general pattern of increased cloud cover near the offshore edge of the gridded area and

[2]Weiss, G., Fundaçao Universidade do Rio Grande, Rio Grande, Brazil.

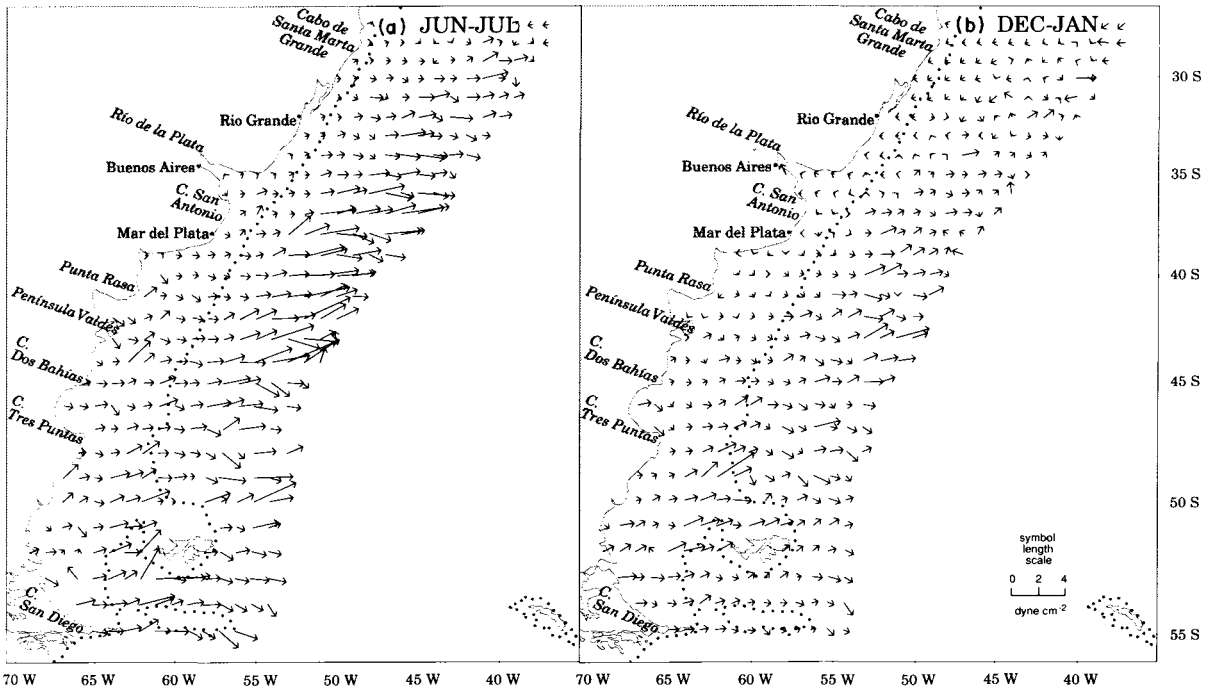

Figure 2. Sea surface wind stress distributions for (a) austral winter (June–July), and (b) austral summer (December–January). A symbol length scale is shown in panel (b). The dotted line indicates the continental shelf limit (200 m isobath).

a local maximum of average cloud cover (> 70%) situated just north of the Falklands. The entire near-coastal region from Rio Grande (~ 32°S) to Península Valdéz (~ 43°S) appears as an area of rather minimal cloud cover during summer, with two large areas of less than 45% average cloud cover being separated by a band of slightly more than 45% which extends northeastward from the offshore region to intersect the coast near Mar del Plata (~ 35°–38°S).

The summer pattern of solar radiation (Fig. 3d) available for absorption, either by water molecules to warm the upper ocean or by plant pigments to support organic production, is strongly affected by the cloud cover distribution. The vicinity of the Falkland Islands receives the lowest solar radiation in the region. The anchoita habitat, near the coast, receives a relatively larger flux of solar radiation entering the ocean than does the area further offshore.

Sea-surface temperature

The pattern of sea-surface temperature (Fig. 4) is dominated by the major boundary flows of the region. These advective effects are large enough so that, other than the global-scale poleward temperature decrease, effects of the pattern of direct solar heating (Fig. 3b, d) are effectively masked. The effect of the warm poleward-flowing Brazil Current is seen in the tongue-like southwestwardly contortions of the isotherms in the northern portion of the region. Oppositely orientated tongue-like features mark the cold equatorward-flowing Falkland Current which dominates the pattern in the mid-portion of the gridded region. There is an impression of a "collision" of these two massive boundary current flows in the area off the Río de la Plata (Gordon and Greenglove, 1986; Olson *et al.*, 1988), with the Brazil Current flow being deflected offshore and the Falkland Current appearing to slide inshore of the Brazil Current to take on the character of a coastal counterflow. Also, inshore of the Falkland Current various instances of recurvature of the isotherms, particularly in the area of ~ 40°S to ~ 45°S latitude, suggest some degree of coastal counterflow in the poleward direction over the mid-shelf.

Wind mixing index

We estimate the intensity of input of mechanical energy by the wind, which would then become available for turbulent mixing of the upper ocean, by means of a "wind mixing index", which is the mean value of the third power (cube) of the wind speed (see Appendix). In our region of interest (Fig. 5), values of this index are very much higher in the offshore region than in the band lying within several hundred kilometers of the coast. A local maximum tends to

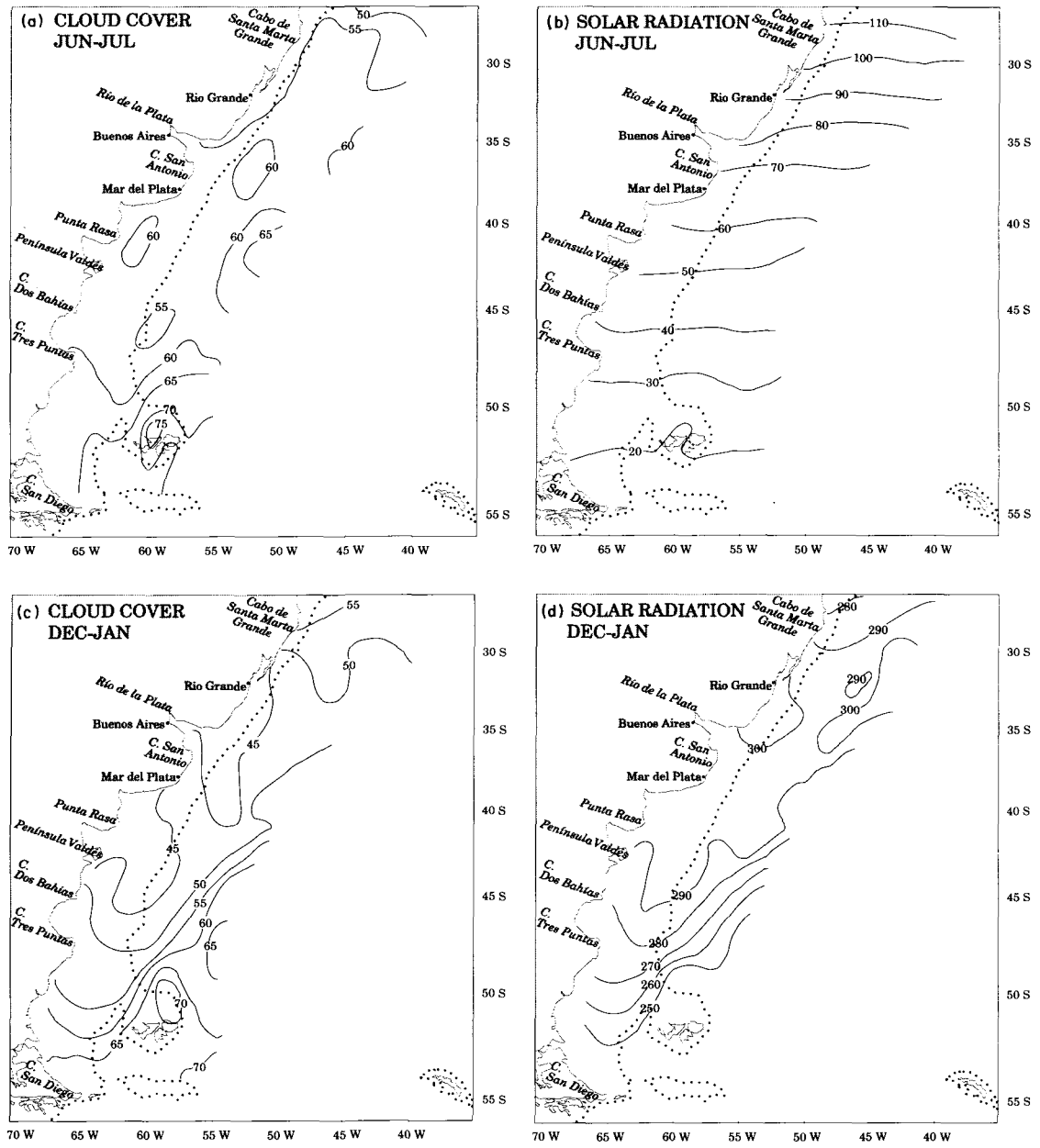

Figure 3. Mean cloud cover and solar radiation. (a) Cloud cover during June–July (austral winter); (b) solar radiation absorbed through the sea surface during June–July; (c) cloud cover during December–January (austral summer); (d) solar radiation absorbed through the sea surface during December–January. Units for cloud cover distributions are percent of sky obscured. Units for solar radiation distributions are watts m^{-2} (to convert to cal cm^{-2} day^{-1}, multiply by the factor 2.064). The dotted line indicates the continental shelf limit (200 m isobath).

be found in the latitude band from about 38° to 45°S, about 600 km offshore. Parrish *et al.* (1983) found that, with the exception of the South African population, the major anchovy populations of eastern ocean boundary regions (e.g. the anchoveta of north-central Peru, the anchoveta of southern Peru and northern Chile, the anchovy of Namibia, and the anchovy of the Southern California Bight) spawn under circumstances such that seasonal average wind mixing index values exceeding about 0.3 index units (one wind mixing index unit = 1000 m^3 s^{-3}) are avoided. Such low seasonal values of the index are generally absent off subtropical eastern South America, except perhaps in restricted areas directly sheltered by coastal topography. On the scales resolved by our one-

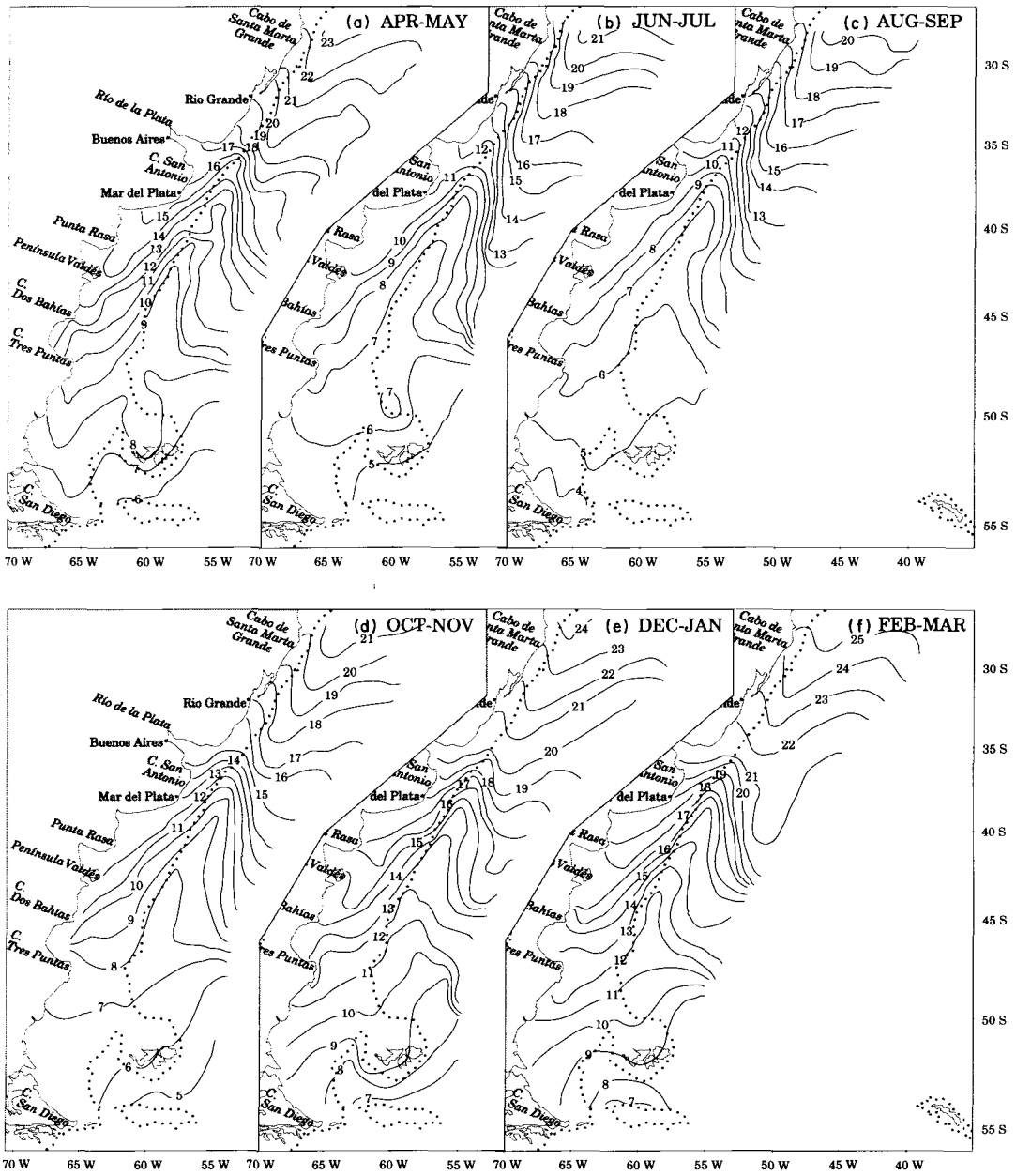

Figure 4. Sea surface temperature distributions for two-month segments of the seasonal cycle. Units are degrees Celsius. The dotted line indicates the continental shelf limit (200 m isobath). (a) April–May; (b) June–July; (c) August–September; (d) October–November; (e) December–January; (f) February–March.

degree areal summaries, minimum index values near the coast tend to fall only slightly below 0.5.

From late fall to early spring (Fig. 4a, b, c) the area within the 0.5 wind mixing index contour tends to be restricted to the far north of the region or to within the mouth of the Río de la Plata. However, during spring (Fig. 5d) the 0.5 contour encompasses an area off the stretch of coastline from near Rio Grande (~32°S) to somewhat southwest of Mar del Plata. To the south of Punta Rasa (~41°S) it reappears, encompasses Península Valdéz, and extends to the vicinity of Cabo Dos Bahías (~45°S). During early summer (Fig. 5e) the southward extremity (except for a disjoint segment south of Cabo Tres Puntos) of the 0.5 index value contour recedes northward to Península Valdéz (~43°S). By late summer to early fall (Fig. 5f), the area where seasonal values of the

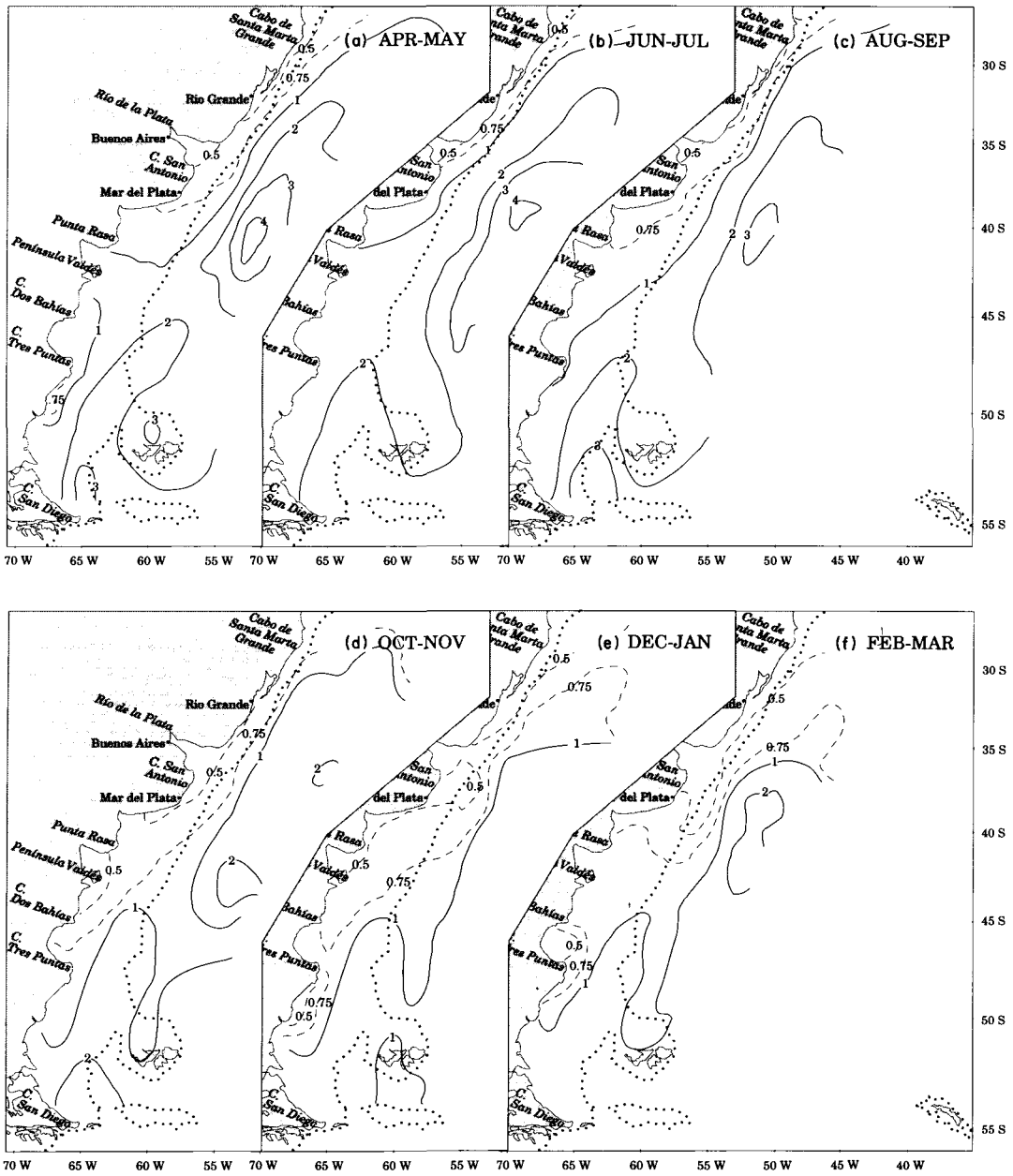

Figure 5. "Wind cubed" index of rate of addition to the ocean, by the wind, of mechanical energy available for turbulent mixing of the upper water column; nominal units are $m^{-3} s^{-3}$. The dotted line indicates the continental shelf limit (200 m isobath). (a) April–May; (b) June–July; (c) August–September; (d) October–November; (e) December–January; (f) February–March.

wind mixing index are less than 0.5 has receded northward along the coast such that its southern limit lies near Mar del Plata (~38°S).

Subsurface stability structure

Except within the interior of the coastal bight (herein called the "Southeastern Brazilian Bight", after Matsuura, 1989) to the north of Cabo Santa Marta Grande (see Fig. 4 in BP), seasonal mixing index values substantially lower than 0.5 tend not to be available in the habitat of the anchoita. Thus, although the southerly extent of the anchoita's spawning habitat expands and contracts roughly in phase with the seasonal movement of the zone of relatively low wind mixing energy, spawning must largely take place at much higher rates of wind-derived mixing energy than the 0.05–

0.3 index values typical of anchovy reproductive habitats in eastern ocean coastal ecosystems (Parrish *et al.*, 1983). The only comparable example among the anchovy populations treated by Parrish *et al.* is the South African anchovy population, where index values exceeding 0.6 characterize the spawning habitat. Parrish *et al.* attribute the ability of the South African population successfully to reproduce under such energetic wind conditions to a protected stable layer formed at depth by the confluence of warm Indian Ocean surface water from the Agulhas Current with the cooler, more dense Atlantic source water of the Benguela Current (see also Shelton and Hutchings, 1990).

Off eastern South America, there exists a similar confluence of the warm tropical Brazil Current with the cool Falkland Current (Olson *et al.*, 1988), although the anchoita reproductive habitat extends far beyond the area directly affected by this confluence. To demonstrate characteristic subsurface structure in various areas of the habitat, we have assembled some schematic profiles of subsurface structure (Fig. 6) from available published sections (see caption for sources). These are constructed from contoured sections rather than from original data and in most cases are derived from a single cruise rather than a long-term climatological mean. We thus offer them merely as illustrations of the general types of structure to be found in particular regions and seasons.

During summer within the Brazilian Bight (Fig. 6a, c), very strong stability is built up in the upper water column by intrusion of deeper waters which upwell and spread across the continental shelf (Castro Filho *et al.*, 1987) and by surface heating and lack of turbulent mixing, particularly in the shoreward portion of the bight (Fig. 6a). Thus, during the late spring to early summer period there is strong stability and resistance to vertical mixing of the water column. Conversely, during winter the water in the shoreward half of the bight may be completely homogenized (Fig. 6b).

Off Uruguay and the extreme south of Brazil, subsurface stability over the continental shelf is strongest in the winter (Castello and Müller, 1977) due in large part to freshwater runoff from the continent; apparently, salinity controls the density structure to such an extent that at some locations on the shelf, temperature actually increases with depth during winter (Fig. 6f). Sizable winter spawning occurs in this region (Fig. 1). In addition, during the other seasons of the year, there continues to be substantial stability in the water column structure (e.g. Fig. 6e) as well as heavy spawning activity, which apparently (there are no published summer surveys) continues throughout the year.

Further south along the Argentine coast the situation reverses. Water column stability is strongest in summer (Fig. 6g) and may vanish completely in winter (Fig. 6h). Here spawning declines sharply during winter. However, in addition to poor stability conditions, the temperature in this region during winter (Fig. 6h) may fall below a level favorable for reproductive activity of *Engraulis* (see Discussion).

The Patagonian shelf, yet further to the south, is characterized by strong tidal mixing which in shallower areas may homogenize the whole water column. The result is occurrence during summer of shelf sea fronts (Simpson and Hunter, 1974; Hunter and Sharp, 1983), which are zones of convergence between mixed water on the shallower side (Fig. 6i) and stratified water offshore (Fig. 6j). Fronts of this type are strongly evident near Península Valdéz (Glorioso, 1987).

Surface Ekman transport

The seasonal progression of bimonthly distributions of surface Ekman transport, which represents the transport in the ocean surface layer responding to the seasonal variablity of wind stress (see Appendix), is displayed in Fig. 7. Strong surface convergence in a band from about 300 to 600 km offshore, due to the anticyclonic wind stress curl discussed in the subsection on wind stress, is obvious in the general decrease in vector symbol length in the direction of transport. The existence of surface convergence in the offshore area is in distinct similarity to eastern boundary current regions where anticyclonic wind stress curl at similar distances offshore (Nelson, 1977; Bakun and Nelson, 1991), and corresponding convergence of surface waters and organisms may provide particularly efficient feeding grounds for nektonic predators (Parrish *et al.*, 1981). Offshore of the convergent area there appears to be general divergence in the surface Ekman transport field.

Near the coast, the surface Ekman transport is generally directed toward shore, and so organisms of this region appear to be largely unaffected by the problem of chronic offshore Ekman transport of planktonic stages that seems to be a controlling aspect of spawning strategies in eastern boundary regions (Parrish *et al.*, 1981, 1983) or even in the more tropical region of the western South Atlantic (Bakun and Parrish, 1990). In fact the only incidence of substantial large-scale average offshore Ekman transport is from Cabo Santa Marta Grande (~28°S) to Rio Grande (~32°S) during the warmer half of the year (Fig. 7d, e, f). As noted earlier, there appears to be reduced anchoita spawning activity in the northern part of the range during summer and fall. This absence of the large-scale wind-driven offshore loss of reproductive products that is faced by pelagic spawners in upwelling systems is another feature in common with South African anchovies (*Engraulis capensis*) which migrate out of the Benguela upwelling system as young adults to join a spawning population positioned in an area adjacent to the Cape of Good Hope, where Ekman transport is characteristically directed toward the coast (Parrish *et al.*, 1983).

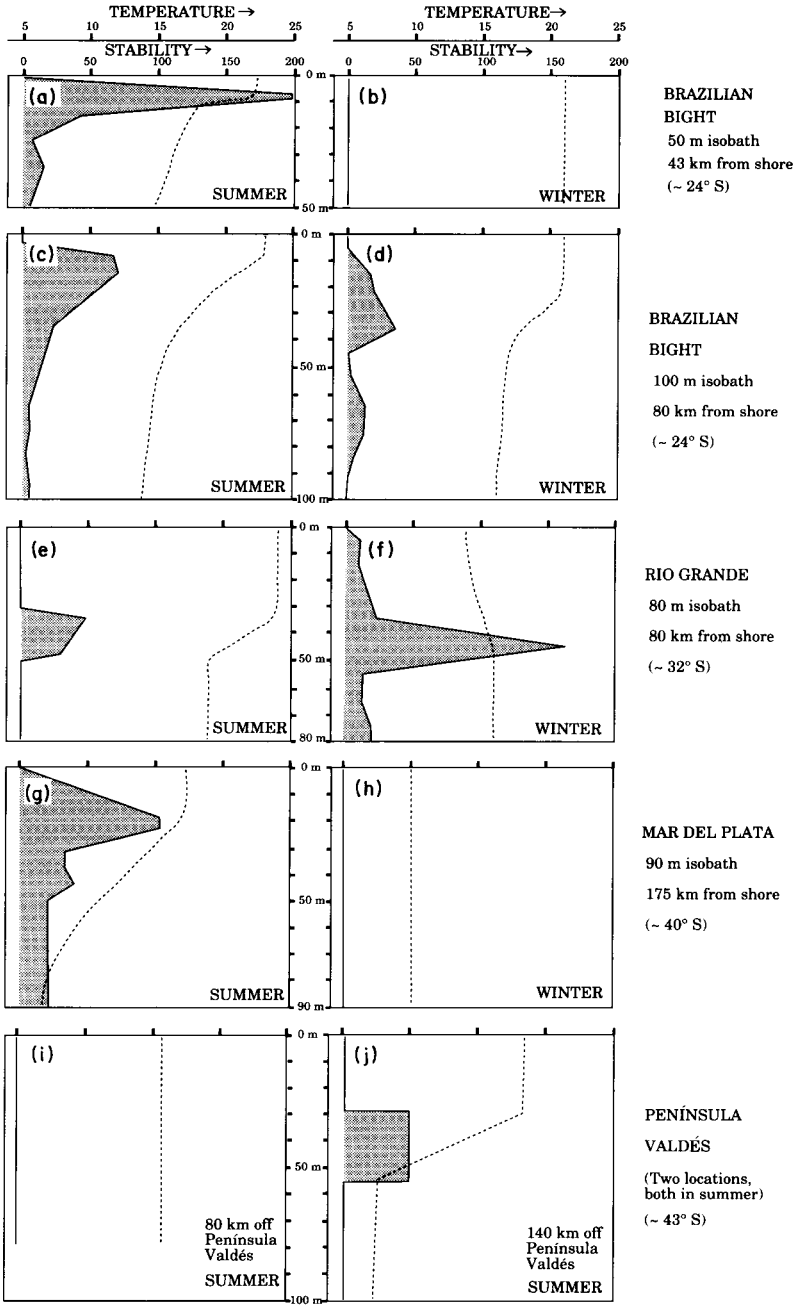

Figure 6. Vertical distributions of static stability ($10^{-3}d\sigma_t/dz$; m^{-1}) plotted as a solid line with shading, and temperature (°C) plotted as a dashed line. These distributions were drawn from published contoured profiles rather than from original data: (a, b, c, d) from Castro Filho *et al.* (1987); (e, f) from Castello and Müller (1977); (g, h) from Martos (1986); (i, j) from Glorioso (1987). Glorioso presented only temperature profiles; thus effects of salinity structure are neglected in panels (i) and (j).

Processes of nutrient enrichment

The only area within the anchoita habitat where sustained, locally wind-driven coastal upwelling occurs is the Cabo Frio–Cabo São Tomé upwelling center (described in BP) at the northern limit of the Brazilian Bight. The existence of enclosed gyral circulation patterns within the coastal indentation favors diffusion of the enriched surface waters, originating at the upwelling center, into the Bight area. In addition, vertical sections (e.g. Castro Filho *et al.*, 1987) suggest continued upwelling near the shelf break along the seaward boundary of the Bight area where frictional drag

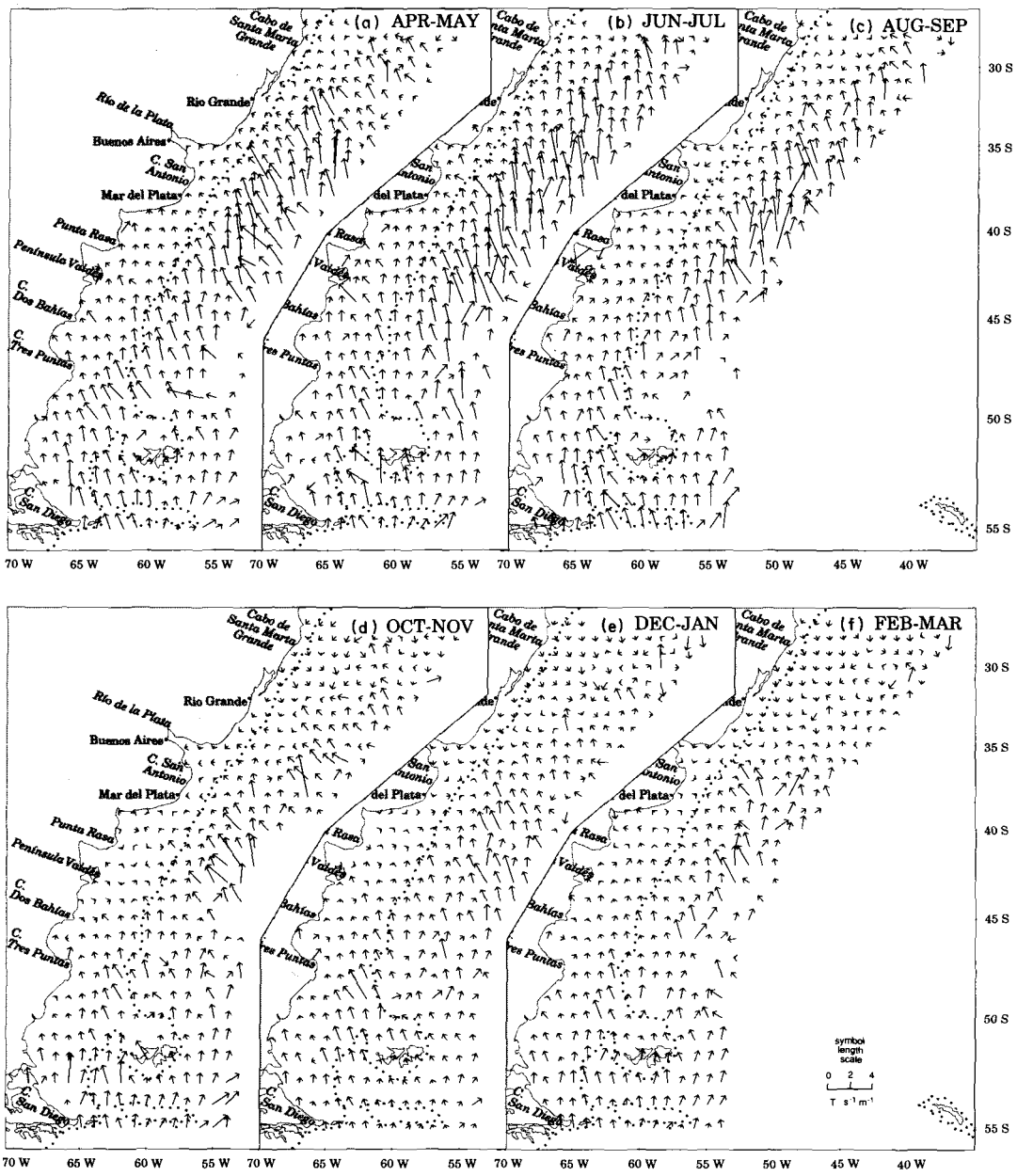

Figure 7. Surface Ekman transport distributions for two-month segments of the seasonal cycle. Transport is proportional to vector symbol length. A symbol length scale is provided (panel g); units are metric tonnes per second across each meter width. The dotted line indicates the continental shelf limit (200 m isobath). (a) April–May; (b) June–July; (c) August–September; (d) October–November; (e) December–January; (f) February–March.

created by the Brazil Current flowing along the shelf edge would lead to locally subgeostrophic flow, a correspondingly unbalanced onshore–offshore pressure gradient, and resulting onshore transport in a bottom Ekman layer (Hsueh and O'Brien, 1971). During the austral spring and summer, there is also substantial wind-driven offshore Ekman transport at the seaward edge of the Bight area (see Fig. 3 in BP) available to drive wind-induced upwelling occurring at the shelf break (Huyer, 1976; Petrie, 1983).

To the south (i.e. in the bulk of the anchoita habitat), seasonal-scale offshore-directed wind-driven surface transport that would drive conventional coastal upwelling is largely lacking (Fig. 7), except for minimal amounts during summer extending only as far south as Rio Grande

(~32°S). However, shelf break upwelling continues to be highly evident in vertical hydrographic sections (e.g. Servicio de Hidrografía Naval, 1969) and in satellite imagery (Podesta, 1990), even in the area dominated by the northward flowing Falkland Current. Ekman transport near the sea floor due to bottom drag in such an equatorward western boundary current would be directed offshore, rather than in the onshore direction corresponding to upwelling. Podesta cites several potential mechanisms for shelf break upwelling in such a case. These include upwelling in small-scale eddies along the current edge (Paffenhöffer *et al.*, 1984), interactions between coastal trapped waves and bottom topography (Dickson *et al.*, 1980), and effects of interactions of internal tides with the shelf break and wind stress (Mazé *et al.*, 1986). In addition, Kinsella *et al.* (1987) describe a mechanism for onshore water movement in response to the Ekman suction caused by curl of the bottom stress in an equatorward western boundary flow.

Finally, tidal mixing over the shelf can have a similar effect to upwelling. In the resulting homogenized water column, nutrients and other properties associated with the denser lower layers of the previously stratified water are mixed into the illuminated upper layers where they are available for photosynthesis. Carreto and Benavides (in press) cite consistently greater availability of nitrates in the euphotic zone on the mixed side of the fronts near Península Valdéz, compared to the stratified side. They also note predominance of chain-forming diatoms (such as typify upwelling centers) on the mixed side and relative scarcity of phytoplankters (being mostly heterotrophic dinoflagellates) on the stratified side. They report that the largest phytoplankton concentrations occur in the transition zone between (i.e. associated with the convergent front). Based on studies of satellite imagery, Podesta (1990) states that the area influenced by these fronts, and also the area of the shelf-break front, are the only places on the Patagonian shelf where near-surface phytoplankton biomass remains high throughout the summer.

Discussion

The anchoita spawning habitat extends some 2800 km along the coast of South America (Fig. 1) and spans a broad range of environmental conditions. The range of actual[3] sea surface temperature (SST) at which *Engraulis* eggs occur is from 8.8°C to 23.2°C in Argentine waters (Sánchez, 1989), and from 16°C to 28°C in the Southeastern Brazilian Bight (Nakatani, 1982). This is similar to the overall range found in the California Current, 9°C to 27°C (Hernandez-Vasquez, 1991). According to Sánchez (1989) the temperature corresponding to maximum spawning incidence of *Engraulis* varies from 13.0°C in September to 18.5°C in February in Argentine waters; the corresponding values for California Current *Engraulis* are from 14.5°C in April to 18.7°C in September (Hernandez-Vasquez, 1991).

Most sampling of pelagic larvae is done via vertically integrating "oblique" tows, but occurrence or absence is usually, as in the studies cited above, compared to SST. Where there is a marked vertical temperature structure, SST may be a rather imprecise indicator of the temperature conditions in the depth zone actually occupied by the sampled larvae. Campaner and Honda (1987) state that in the Brazilian Bight (~23°–27°S) late winter anchoita spawning is scattered throughout the outer shelf where temperatures at depth are less than 20°C, whereas during the late spring to early summer, spawning is concentrated in cool upwelling regions south of Cabo Frio and near the coast. In the same region, Matsuura *et al.* (1985) found nearshore concentrations of adult anchovy in cool (15–20°C) upwelled water; in areas with a higher SST, anchovies were found in or beneath a shallow thermocline at temperatures of 15–19°C. Brewer (1976) determined temperature tolerances of larvae of California Current northern anchovy (*Engraulis mordax*) by controlled laboratory experiments. He found that some eggs hatch at any temperature between 8.5° and 28.5°C and that the larval temperature tolerance range extends from 7° to 30°C. However, the proportion of larvae which developed in a normal manner decreased when temperatures fell below 11.5°C or exceeded 27°C.

From the information available, the reproductive habitat temperature tolerance of *Engraulis anchoita* does not therefore appear to differ substantially from that of eastern ocean boundary region populations of the genus *Engraulis*. In fact, the spawning habitat temperature range of this one species, in terms of long-term seasonal mean SST, essentially encompasses the combined temperature ranges of all the eastern ocean populations examined by Parrish *et al.* (1983). Therefore, we find in the case of the anchoita no reason to modify the conclusion, reached by Parrish *et al.* (1983) with respect to eastern ocean anchovies (and also sardines), that selection of spawning habitat for any particular optimum temperature may be less important than the striking of a beneficial balance of physical processes affecting water column stability, retention of reproductive products within a favorable habitat, and nutrient enrichment leading to adequate production of appropriate larval food particles.

The most common manner of striking this balance, noted by Parrish *et al.*, is in an environmental configuration wherein spawning grounds are located within coastal indentations downstream of coastal upwelling centers. The upwelling provides enrichment to the food web, the products of which diffuse into the coastal bight where the strong offshore Ekman transport characteristic of

[3]As opposed to long-term seasonal mean values, as displayed in Fig. 4.

upwelling regions relaxes and semi-enclosed gyral circulation patterns aid retention of larvae within the bight area. Due to the sheltering effect of the coastal topography, wind-mixing falls to very low values within these indentations, allowing formation of the fine-scale food particle concentrations favoring successful larval feeding. The archetype of this pattern is the Southern California Bight, which constitutes the major spawning grounds of the northern anchovy (*Engraulis mordax*) and also, prior to its population collapse, of the Pacific sardine (*Sardinops sagax caerulea*). This pattern also applies in more or less degree to the anchoveta (*Engraulis ringens*) and sardine (*Sardinops sagax sagax*) populations spawning off southern Peru and northern Chile, to the sardine (*Sardina pilchardus*) stocks of the Canary Current system spawning in coastal bights near Casablanca and near Ifni, and to the anchovies (*Engraulis capensis*) and sardines (*Sardinops sagax ocellatus*) spawning near Palgrave Point in Namibia.

Bakun and Parrish (1990) show a nearly identical configuration (Fig. 8a) for the spawning habitat of the Brazilian sardine (*Sardinella aurita*), a sardine-type fish of a more tropical genus than the *Sardinops* and *Sardina* species inhabiting subtropical eastern ocean upwelling systems. This population shares the Brazilian Bight spawning habitat with the northernmost segment of the anchoita population.

In the bulk of the anchoita habitat to the south, this particular configuration is not available. Surface Ekman transport tends to be directed onshore (Fig. 7), which is opposite to the direction that would induce coastal upwelling. However, the hydrographic situation of this wide, abruptly breaking continental shelf generates substantial upwelling at the shelf break (see previous section). The onshore Ekman transport would serve to carry the upwelling-based nutrients and enriched production onto the inner shelf habitat, where the continent itself serves as a shield from the large-scale westerly winds and relatively low wind-mixing rates result (Fig. 5). Under these conditions, relatively strong water column stability (Fig. 6e, f, g) is favored by confluence of different water masses associated with the various alongshore boundary flows, by strong seasonal surface heating in the wind sheltered region, and by substantial fresh water input. South of Mar del Plata, where water column stability disappears during winter (Fig. 6h), no substantial winter spawning is reported, although as discussed above we cannot isolate this finding from a possible effect of temperature. The areas of water mass confluence, including fronts associated with the freshwater outflows, represent convergence zones which may serve to concentrate distributions of larval food particles. Certainly the onshore-directed surface Ekman transport facilitates the retention of eggs and larvae within the shelf habitat. Thus, it appears that in quite a different configuration (Fig. 8b) to the common one for upwelling regions (Fig. 8a), the various processes combine to yield quite similar conditions for successful reproduction. This second configuration would seem to have its strongest analog in the spawning grounds of the South African anchovy population (Parrish *et al.*, 1983).

Toward the southern end of the reproductive habitat of the anchoita, notably in the vicinity of Península Valdéz (see previous section), strong tidal mixing over the very wide Patagonian shelf results in a third configuration (Fig. 8c). Over the shallower areas, tidal energy is sufficient to overcome the potential energy of the stratified water column and the water may become mixed from top to bottom. Nutrients that otherwise would have been held in the denser bottom layer are mixed upward into the illuminated surface layers to support photosynthetic production. In the homogenized area, the mixed water column is more dense at the surface and less dense at depth compared to water at the same depth in the stratified area offshore. Thus, surface water from the stratified region would tend to override the heavier mixed water, resulting in shoreward surface flow toward a convergent front at the sea surface; the mixed water would tend to sink under the front and flow offshore beneath the surface layer (Fig. 8c). At the bottom, the more dense water from offshore would tend to push shoreward to displace the less dense mixed water. These interleaving flows of different densities form a stable thermocline layer flowing slowly offshore from the frontal zone.

Within this mid-depth layer, the several conditions common to the other two configurations (i.e. those illustrated in Fig. 8a and b) would appear to be well realized. Flow from a zone of enrichment (the mixed zone) may carry resultant production of food particles (e.g. developmental stages of calanoid copepods which appear to be the principal dietary items of both larval and juvenile anchoita (Ciechomski, 1967)) into a zone of stability (the mid-depth thermocline). Convergence within the frontal zone may intensify formation of concentrated patch structure, which is buffered from turbulent dispersion due to tidal friction at the bottom by the denser layer beneath and from wind-generated turbulence by the less dense layer above. Retention of larvae within the coastal habitat may be aided by appropriate vertical migratory behavior. For example, excursion into either the upper layer or the lower layer, either on a diel basis or in the course of ontogenetic development, would tend to counter the general offshore movement within the mid-depth layer (Bakun, 1989). Whether or not adaptive vertical migration is actually involved, the Patagonian shelf is so wide (more than 350 km in width off Península Valdéz) that the layered circulations associated with shelf sea fronts near the coast must surely decay within a small fraction of the total distance to the offshore limit of the continental shelf habitat. The large-scale onshore wind-driven Ekman transport, tending to impede drift off the shelf, becomes abruptly stronger with distance from the coast (Fig. 7).

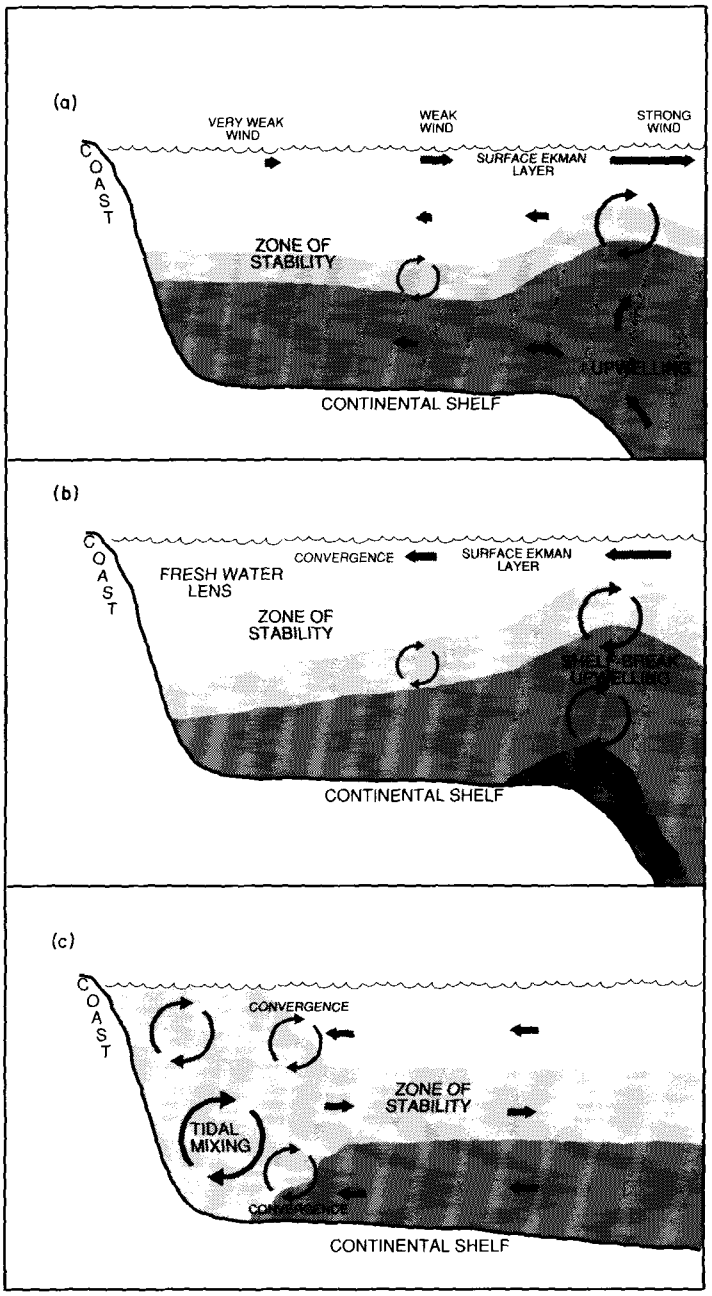

Figure 8. Schematic diagrams of environmental configurations prominent in spawning strategies of *Engraulis anchoita*. Heavier shading connotes greater water density. Wider arrows indicate mean water transport; lengths are scaled to suggest relative magnitudes. Linked circular pairs of arrows indicate mixing processes; their sizes are scaled to suggest relative intensities of mixing: (a) Within a coastal indentation in a wind-driven coastal upwelling regime (i.e. the Brazilian Bight; also descriptive of the Southern California Bight in the northeastern Pacific and other eastern ocean anchovy habitats). (b) Onshore wind-driven transport over a wide continental shelf with upwelling at the shelf break and freshwater runoff from the continent (i.e. extreme north coast of Argentina, coast of Uruguay and Brazilian coast to north of Rio Grande). (c) A shelf-sea front system driven by tidal mixing (i.e. the Patagonian shelf in the vicinity of Península Valdéz; also descriptive of similar frontal systems in the North Sea, the Gulf of Maine, etc.)

This third configuration (Fig. 8c) has been previously indicated (Iles and Sinclair, 1982; Sinclair, 1988) as being prominent in the spawning habitat of herring (*Clupea*) in high latitude shelf-seas such as the Gulf of Maine, the North Sea, etc. Also, Buckley and Lough (1987) report that haddock larvae (*Melanogrammus aeglefinus*) are

found to be much more numerous and faster growing in the thermocline zone immediately offshore of the tidally-mixed area over Georges Bank than in either the surface waters or at any depth within the mixed area.

Conclusions and speculative remarks

The example of the anchoita thus demonstrates the extreme versatility of anchovies. Evidently, one extended population encompasses the combined reproductive temperature ranges of all the eastern ocean populations examined by Parrish *et al.* (1983). It also uses both classes of environmental configurations shown in that study as fostering successful anchovy reproduction in eastern ocean ecosystems. In addition, in the very wide Patagonian shelf habitat, the anchoita evidently utilizes a configuration similar to one used by herring in the wide shelf-sea ecosystems of boreal high latitudes. The anchoita is also successful in substantially co-inhabiting, by partitioning habitat space according to temperature preference, the spatial area which constitutes the primary habitat of the Brazilian sardine, a more tropical species.

One might speculate whether this evident "plasticity" with respect to external conditions could be a major reason for the remarkable success of the genus *Engraulis* worldwide. For example, the anchoveta (*Engraulis ringens*) of the Peru Current was, before exploitation, by far the largest single fish population ever known to inhabit a coastal ecosystem. It also appears to have largely remained the overwhelmingly dominant component of the Peru Current ecosystem for millennia (DeVries and Pearcy, 1982), rather than to have suffered periodic displacement by the somewhat longer-lived sardines, as apparently has occurred in other systems (Soutar and Isaacs, 1969; Shackleton, 1987). We might note that the recent expansion of sardines in the Peru Current system came only after enormous exploitation had contributed to the collapse of the anchoveta population. An explanation for the spectacular success of the anchoveta might be the very fact that the Peru system, being geographically situated so as to bear the full brunt of global scale El Niño–Southern Oscillation phenomena, is uniquely subject to intermittent drastic environmental rearrangement. These disruptions could give the advantage to the Peruvian anchoveta over more specialized (e.g. demersal) species which are able to establish and maintain themselves in other ecosystems, feeding at a somewhat higher trophic level (i.e. less efficiently with respect to the primary organic production of the ecosystem) than anchovies, while suppressing the growth of lower trophic level populations through their incessant predation. In an ecosystem relatively free of such less productive predatory components, much larger biomasses might be attained by a low trophic level species having a short life cycle and rapid population responses.

In summary, our various examinations of seasonality and geography of anchovy reproductive activity have yielded a rather consistent picture of quite a simple combination of environmental factors. First, we consistently find enhanced enrichment of the food web via physical processes (upwelling, etc.). Second, there is opportunity for concentrated patches of food particles to accumulate (i.e. by means of stability, lack of active turbulent mixing, and/or strong convergence in frontal structures). Finally, there is available some mechanism promoting retention of reproductive products within the near-coastal habitat. Areas where this combination does not exist, such as directly within "core" zones of maximal coastal upwelling, appear to be avoided in anchovy spawning habits. Any coastal marine ecosystem having an appropriate balance of this combination of factors, as long as temperature and other physiological factors fall within the species tolerances, would seem to be an appropriate habitat for a substantial anchovy population. Exceptions may be systems where long-period temporal irregularity may be mild enough to allow more specialized species to gain the upper hand. Likewise, in systems characterized by large-scale spatial irregularity (i.e. where the combination of factors supporting successful reproduction may exist in only limited subareas), the advantage may shift toward species more adapted for migration between adult feeding grounds and the reproductive habitat. One might speculate that the California Current system, where pelagic fishes spawn mainly within the Southern California Bight but migrate long distances to adult feeding grounds (Parrish *et al.*, 1981), might tend toward this latter situation. In the California system the more migratory sardines appear often to have been dominant over anchovies (Shackleton, 1987).

Off subtropical eastern South America, we see appropriate combinations of the several factors spread, in several different configurations, over a vast stretch of coastal ocean habitat. Accordingly, *Engraulis anchoita* dominates its trophic level in the coastal ecosystem of the southeastern Atlantic over the entire latitude band where temperatures are within its physiological tolerances. However, because various factors, including the very wide continental shelf area, relative absence of strong environmental perturbation, less dispersion than in certain other systems, etc., allow maintenance of large populations of predators (hake, squid, etc.), the anchoita itself may not approach the maximum total biomass that has been achieved by its relative on the western side of the continent. However, it is without question a key component of the trophic structure of this vast and enormously rich shelf-sea ecosystem.

Acknowledgements

This work could not have been completed without the help and local knowledge of colleagues in Argentina and Brazil. We particularly want to thank D. A. Bertone, J. P.

Castello, J. D. Ciechomski, M. B. Cousseau, J. Hansen, K. Nakatani, Y. Matsuura, M. C. Piccolo, S. A. Saccardo, R. P. Sánchez, H. J. Spach, and G. Weiss. We also acknowledge the help we received from discussions with students, staff, and faculty of the Instituto Oceanográfico do Universidade de São Paulo, the Fundaçao Universidade do Rio Grande, the Instituto Argentino de Oceanografía, and the Instituto Nacional de Investigación y Desarrollo Pesquero. In addition, we benefited greatly from conversations with G. Podesta of the University of Miami. We also thank C. M. Antoinette Nichols, who produced the illustrations, and Art Stroud, who summarized the historical maritime report files.

References

Bakun, A. 1985. Comparative studies and the recruitment problem: Searching for generalizations. CalCOFI Rep., 26: 30–40.

Bakun, A. 1989. L'ocean et la variabilité des populations marines. *In* L'Homme et les Écosystems Halieutiques, pp. 155–187. Ed. by J. P. Troadec. IFREMER, Brest. 817 pp.

Bakun, A., and Nelson, C. S. (1991) The seasonal cycle of wind stress curl in subtropical eastern boundary current regions. J. Phys. Oceanogr. (In press, Sept. 1991 issue).

Bakun, A., and Parrish, R. H. 1982. Turbulence, transport, and pelagic fish in the California and Peru Current systems. CalCOFI Rep., 23: 99–112.

Bakun, A., and Parrish, R. H. 1990. Comparative studies of coastal pelagic fish reproductive habitats: the Brazilian sardine (*Sardinella aurita*). J. Cons. int. Explor. Mer., 46: 269–283.

Brewer, G. D. 1976. Thermal tolerance and resistance of the northern anchovy *Engraulis mordax*. Fish. Bull. US, 74: 433–445.

Buckley, L. J., and Lough, R. G. 1987. Recent growth, biochemical composition, and prey field of larval haddock (*Melanogrammus aeglefinus*) and Atlantic cod (*Gadus morhua*) on Georges Bank. Can. J. Fish. aquat. Sci., 44: 14–25.

Companer, A. F., and Honda, S. 1987. Distribution and co-occurrence of *Calanoides carinatus* and larvae of *Sardinella braziliensis* and *Engraulis anchoita* over the southern Brazilian continental shelf. Bolm. Inst. oceanogr., S. Paulo, 35(1); 7–16.

Carreto, J. I., and Benavides, H. R. 1989. Phytoplankton. *In* Annex V, Synopsis on the reproductive biology and early life history of *Engraulis anchoita* and related environmental conditions in Argentine waters, pp. 2–3. Second IOC Workshop on Sardine/Anchovy Recruitment Project (SARP) in the Southwest Atlantic. IOC Workshop Report, 65. Unesco, Paris.

Castello, J. P. 1989. Synopsis on the reproductive biology and early life history of *Engraulis anchoita* and related environmental conditions in Argentine waters. Annex VII, 7 pp. *In* Second IOC Workshop on Sardine/Anchovy Recruitment Project (SARP) in the Southwest Atlantic. IOC Workshop Report, 65. Unesco, Paris.

Castello, J. P., and Müller, O. O., Jr. 1977. Sobre as condições oceanográficas no Rio Grande do Sul. Atlântica, 2(2): 25–110.

Castro Filho, B. M. de, Miranda, L. B. de, and Miyao, S. Y. 1987. Condições hidrográficas na plataforma continental ao largo de Ubatuba: variações sazonaiss e em média escala. Bolm Inst. Oceanogr., São Paulo, 35(2): 135–151.

Ciechomski, J. D. de. 1967. Investigations on food and feeding habits of the Argentine anchovy *Engraulis anchoita*. CalCOFI Rep., 11: 72–80.

Ciechomski, J. D. de, and Sánchez, R. P. 1986. Problematica del estudio de huevos y larvas de anchoita (*Engraulis anchoita*) en relacion con la evolucion de sus efectivos pesqueros. I Resena de viente anos de investigacion. Publ. Com. Tec. Mix. Fr. Marl. 1(1): 93–109.

Cury, P., and Roy, C. 1989. Optimal environmental window and pelagic fish recruitment success in upwelling areas. Can. J. Fish. aquat. Sci., 46: 670–680.

DeVries, T. J., and Pearcy, W. G. 1982. Fish debris in sediments of the upwelling zone off central Peru: a late Quaternary record. Deep-Sea Res., 28: 87–109.

Dickson, R. R., Gurbutt, P. A., and Pillai, V. N. 1980. Satellite evidence of enhanced upwelling along the European continental slope. J. Phys. Oceanogr., 10: 813–819.

Ekman, V. M. 1905. On the influence of the earth's rotation on ocean currents. Ark. Mat. Astron. Fys., 2(11): 1–55 (reprinted in J. Cons. int. Expl. Mer, 20(2), 1954).

FAO. 1990. FAO yearbook of fishery statistics, Vol. 66, 1988. Food and Agriculture Organization of the United Nations. 502 pp.

Glorioso, P. 1987. Temperature distribution related to shelf-sea fronts on the Patagonian Shelf. Continental Shelf Res., 7: 27–34.

Gordon, A. L., and Greenglove, C. L. 1986. Geostrophic circulation of the Brazil–Falkland confluence. Deep-Sea Res., 33: 573–586.

Hernandez-Vasquez, S. 1991. Pattern analysis of abundance and geographical distribution of sardine (*Sardinops sagax caerulea*) and anchovy (*Engraulis mordax*) eggs and larvae in the California Current: 1951–1989. PhD thesis, Centro de Investigaciones Cientifica y Educacion Superior de Ensenada, Ensenada, B. C., Mexico.

Hsueh, Y., and O'Brien, J. J. 1971. Steady coastal upwelling induced by an along-shore current. J. Phys. Oceanogr., 1: 180–186.

Hubold, G. 1982. Zur laichökologie der Südwestaltlantischen sardelle *Engraulis anchoita* (Hubbs und Marini, 1935) Dissertation zur Erlangung des Doktorgrades *der Mathematisch-Naturwissenschaftlichen Fakultät* der Christian-Albrechts-Universität zu Kiel.

Hunter, J. R., and Sharp, G. D. 1983. Physics and fish populations: shelf sea fronts and fisheries, pp. 659–682. *In* Proceedings of the expert consultation to examine changes in abundance and species composition of neritic fish resources. Ed. by G. D. Sharp and J. Csirke. FAO Fish. Rep., 291. 1224 pp.

Huyer, A. 1976. A comparison of upwelling events in two locations: Oregon and Northwest Africa. J. Mar. Res., 34: 531–546.

Iles, T. D., and Sinclair, M. 1982. Atlantic herring: stock discreteness and abundance. Science, 215: 627–633.

Kinsella, E. D., Hay, A. E., and Denner, W. W. 1987. Wind and topographic effects on the Labrador Current at Carson Canyon. J. Geophys. Res., 92: 10853–10869.

Lasker, R. 1975. Field criteria for survival of anchovy larvae: the relation between inshore chlorophyll maximum layers and successful first feeding. Fish. Bull. US, 73: 453–462.

Lasker, R. 1978. The relation between oceanographic conditions and larval anchovy food in the California Current: Identification of the factors leading to recruitment failure. Rapp. P.-v. Réun. Cons. int. Explor. Mer., 173: 212–230.

Lasker, R. 1988. Studies on the northern anchovy; biology, recruitment, and fishery oceanography, pp. 24–41. *In* Studies on fisheries oceanography. Proceedings of the 25th Anniversary Symposium "Fisheries and Fishery Oceanography in the Coming Century". Tokyo, 10–13 Nov., 1986, Japanese Society of Fishery Oceanography.

Mantero, G. 1989. Early life history, pp. 3–4. *In* Annex VI, Synopsis on the reproductive biology and early life history of

Engraulis anchoita and related environmental conditions in Argentine waters. Second IOC Workshop on Sardine/Anchovy Recruitment Project (SARP) in the Southwest Atlantic. IOC Workshop Report, 65. Unesco, Paris.

Martos, P. 1986. Dinamica oceanografica en la plataforma continental entre las latitudes de 38 y 42 S. Informe Final de Bece de Iniciación CONICET, Instituto Argentino de Oceanografia, Bahia Blanca, Argentina. 140 pp.

Matsuura, Y. 1989. Synopsis on the reproductive biology and early life history of the Brazilian sardine, *Sardinella braziliensis*, and related environmental conditions. Annex VIII, 8 pp. *In* Second IOC Workshop on Sardine/Anchovy Recruitment Project (SARP) in the Southwest Atlantic. IOC Workshop Report, 65. Unesco, Paris.

Matsuura, Y., Amaral, J. C., Sato, G., and Tamassia, S. T. J. 1985. Ocorrencia de peixes pelagicos e a estrutura oceanografica da regiao entre o Cabo de Sao Tome (RJ) e Cananeia (SP), em Jan-Fev/1979. Ser. Doc. Tecm., PDP/SUDEPE, Brasilia, no. 33, pp. 3–70.

Mayr, E. 1982. The growth of biological thought. Harvard Univ. Press, Cambridge, Mass. 974 pp.

Mazé, R., Camus, Y., and Le Tareau, J.-Y. 1986. Formation de gradient thermiques à la surface de l'océan, au-dessuss d'un talus, par interaction entre les ondes et le mélange dû au vent. J. Cons. int. Explor. Mer., 42: 221–240.

Mendelssohn, R., and Mendo, J. 1987. Exploratory analysis of anchoveta recruitment off Peru and related environmental series, pp. 294–306. *In* The Peruvian anchoveta and its upwelling ecosystems: three decades of change. Ed. by D. Pauly and I. Tsukayama. ICLARM Studies and Reviews 15. Instituto del Mar del Peru (IMARPE), Callao, Peru; Deutsche Gesellschaft fur Technische Zusammenarbeit (GTZ), GmbH, Eschborn, Federal Republic of Germany; and International Center for Living Aquatic Resources Management (ICLARM), Manila, Philippines. 351 pp.

Nakatani, K. 1982. Estudos sobre os ovos e larvas de *Engraulis anchoita* (Hubbs & Marini, 1935) (Teleostei, Engraulidae) coletados na regiao entre Cabo Frio (23°S) e Cabo de Santa Marta Grande (29°S). Masters Thesis. Universidade de Sao Paulo.

Nelson, C. S. 1977. Wind stress and wind stress curl over the California Current. US Dep. Commer. NOAA Tech. Rep. NMFS SSRF-714. 87 pp.

Olson, D. B., Podesta, G. P., Evans, R. H., and Brown, O. B. 1988. Temporal variation in the separation of Brazil and Malvinas Currents. Deep-Sea Res., 35: 1971–1990.

Paffenhöffer, G.-A., Wester, B. T., and Nicholas, W. D. 1984. Zooplankton abundance in relation to state and type of intrusions onto the southeastern United States shelf during summer. J. Mar. Res., 42: 995–1017.

Parrish, R. H., Nelson, C. S., and Bakun, A. 1981. Transport mechanisms and reproductive success of fishes in the California Current. Biol. Oceanogr., 1: 175–203.

Parrish, R. H., Bakun, A., Husby, D. M., and Nelson, C. S. 1983. Comparative climatology of selected environmental processes in relation to eastern boundary current pelagic fish reproduction, pp. 731–778. *In* Proceedings of the expert consultation to examine changes in abundance and species composition of neritic fish resources. Ed. by G. D. Sharp and J. Csirke. FAO Fish. Rep., 291. 1224 pp.

Peterman, R. M., and Bradford, M. J. 1987. Wind speed and mortality rate of a marine fish, the northern anchovy (*Engraulis mordax*). Science, 235: 354–356.

Petrie, B. D. 1983. Current response at the shelf break to transient wind forcing. J. Geophys. Res., 88: 9567–9578.

Podesta, G. P. 1990. Migratory pattern of Argentine hake *Merluccius hubbsi* and oceanic processes in the southwestern Atlantic Ocean. Fish. Bull. US, 88: 167–177.

Roy, C., Cury, P., Fontana, A., and Belvèze, A. 1989. Stratégies spatio-temporelles de la reproductiiion des Clupéidés des zones d'upwelling d'Afrique de l'Ouest. Aquat. Living Res., 2: 21–29.

Sánchez, R. 1989. Annex V. Synposis on the reproductive biology and early life history of *Engraulis anchoita*, and related environmental conditions in Argentine waters. *In* Second IOC Workshop on Sardine/Anchovy Recruitment Project (SARP) in the Southwest Atlantic. Montevideo, Uruguay, 21–23 August 1989.

Servicio de Hidrografía Naval. 1969. Datos y resultados de las Campañas "Pesquería". Pesquería V. Publicaciones del Proyecto de Desarrollo Pesquero No. 10/V. Mar del Plata, Argentina. 100 pp.

Shackleton, L. Y. 1987. A comparative study of fossil fish scales from three upwelling regions. S. Afr. J. mar. Sci., 6: 79–84.

Shelton, P. A., and Hutchings, L. 1990. Ocean stability and anchovy spawning in the southern Benguela Current region. Fish Bull. US, 88: 323–338.

Simpson, J. H., and Hunter, J. R. 1974. Fronts in the Irish Sea. Nature, 250: 404–406.

Sinclair, M. 1988. Marine populations: an essay on population regulation and speciation. University of Washington Sea Grant Program (distributed by University of Washington Press. Seattle and London). 252 pp.

Soutar, A., and Isaacs, J. D. 1969. History of fish populations inferred from fish scales in anaerobic sediments off California. CalCOFI Rep., 13: 63–70.

Spach, H. L. 1990. Estudo comparativo da distrbuicao espac-temporal e de padroes de agregacao de ovos e larvas de *Harengula jaguana, 'Sardinella brasiliensis* (Clupeidae: Osteichthyes) e *Engraulis anchoita* (Engraulidae: Osteichthyes) na costa sudeste do Brasil. PhD Thesis. Universidade de Sao Paulo.

Weiss, G., Fiejo de Souza, J. A., and Santos, A. 1976. Contribuicao ao conheciemento dO ictioplancton marinha da plataforma sul do Brasil, Atlantica, Rio Grande, FURG/BOA, 1(1/2): 7–78.

Weiss, G., and Feijo de Souza, J. A. 1977. Desova invernal de *Engraulis anchoita* na costa sul do Brasil em 1970 e 1976. Atlantic, Rio Grande, 2(2): 5–24.

Appendix

(This Appendix presents the "Methods" section from Bakun and Parrish (1990), slightly modified to apply to the present paper.)

Maritime reports contained in the US National Climatic Center's file of surface marine observations (Tape Data Family – 11) were grouped by one-degree latitude/longitude areal quadrangles and by two-month segments of the calendar year. Estimates of the various quantities of interest were produced from each individual report. The average value of all the estimates in each of these groups of reports was taken as the expected value for the location and two-month seasonal segment. The vector quantities, wind stress and Ekman transport, were averaged by component (vector averaged). The one-degree quadrangles selected for these summaries are centered at intersections of a grid of even whole degrees of latitude and longitude, extending 12 degrees of longitude offshore of the coastal boundary. Editing of the data consisted only of a gross error

check to ensure physically possible values. Wind speeds greater than 50 m s^{-1} ($\sim$100 knots) were discarded as non-representative.

The vector quantities (Figs 2 and 7) are displayed as discrete vector symbols, each value being formed from a data set that is independent of all other one-degree quandrangle and two-month seasonal segments. The standard errors of the means of the respective northward and eastward components of the vector averages have also been plotted and examined in this study. Particularly large standard errors are typical of the estimates in certain offshore portions of the gridded area, reflecting not only very low available data density in that part of the region but also highly energetic variability in actual conditions. The low degree of coherence among spatially adjacent values visible in that area of Figures 2 and 7 should thus be regarded as largely reflecting lack of stability of the estimates rather than as indicating real small-scale spatial differences in characteristic value.

In preparing the contoured maps of the scalar quantities (Figs 3, 4, and 5), some minimal spatial smoothing has been applied. A 3 by 3 gridpoint version of the median smoother (Tukey, 1977) was employed to deal with the intense "bull's-eyes" that largely obscured the underlying significant pattern in the more data-poor offshore areas. However, in cases where this procedure may have removed features which were similarly indicated by directly adjacent independent samples and which were judged to be real after examination of the standard errors of the individual sample means, the contours were subjectively adjusted to re-insert the features. The intention has been to avoid showing features that are determined by only a single estimate (i.e. shown only in one of the two-month, one-degree lat/long sample means).

Wind stress

In estimating the stress of the wind on the sea surface we follow the procedures established by Bakun *et al.* (1974). An estimate of the stress is formed from each wind report according to

$$\vec{\tau} = \rho C_D |\vec{v}| \vec{v} \qquad \text{(A.1)}$$

where $\vec{\tau}$ represents the stress vector, ρ is the density of air (considered constant at 0.00122 gm cm^{-3}), C_D is an empirical drag coefficient (considered constant at 0.0013), $|\vec{v}|$ is the scalar wind speed, and $\vec{v}$ is the vector wind velocity. Reports where the wind direction is coded as "variable" are incorporated as calms (zero wind speed) in the stress summaries (see discussion by Bakun, 1987).

Ekman transport

On the seasonal time scales being addressed, the drift of waters at the sea surface under the direct action of the wind stress is satisfactorily characterized by the simplified idealization known as Ekman transport (Ekman, 1905). The net Ekman transport, $\vec{E}$, integrated over the layer of some several tens of meters beneath the sea surface in which it occurs, is given by

$$\vec{E} = \vec{k} \times \frac{\vec{\tau}}{f} \qquad \text{(A.2)}$$

where $\vec{k}$ is a unit vector directed vertically upward, "$\times$" denotes the vector ("cross") product, τ is the wind stress vector and f is the Coriolis parameter ($f = 2\omega \sin \varphi$) where ω is the angular velocity of the earth's rotation and φ is the latitude (negative degrees in the southern hemisphere). Net Ekman transport is thus directed perpendicularly to the left of the wind stress in the southern hemisphere.

Wind mixing index

The rate at which the wind imparts mechanical energy to the ocean to produce turbulent mixing of the upper water column is roughly proportional to the third power, or "cube", of the wind speed (Elsberry and Garwood, 1978). A "wind mixing index", which is simply the mean of the cube of the observed wind speeds in each of the seasonal/areal samples, provides a guide to the variability in this particular process (Bakun and Parrish, 1982). In this case wind reports with the direction coded as "variable" are handled differently than in the stress summaries. Here the wind speed enters as a scalar quantity and directionality is immaterial, and so the wind speed value is incorporated directly as coded in the report.

Solar radiation

Net incoming solar radiation, Q_s, absorbed by the ocean was estimated from each individual report according to Bakun's (1987) adaptation of Nelson and Husby's (1983) computational procedure. The procedure is based on the standard formulation

$$Q_s = (1 - \alpha) Q_0 (1 - 0.62\,C + 0.0019\,h) \qquad \text{(A.3)}$$

where α is the fraction of incoming radiation reflected from the sea surface, Q_0 is the sum of the direct and diffuse radiation reaching the ground under a cloudless sky, C is the observed total cloud amount in tenths of sky covered and h is the noon solar altitude. Q_0 is estimated according to the procedures and tables presented by List (1949), using a 4×4 element curvilinear interpolation of the table entries via Bessel's central difference formula and assuming the atmospheric transmission coefficient of 0.7 recommended by Seckel and Beaudry (1973). The linear cloud correction in Equation (3) is as suggested by Reed (1977); Reed's recommendation that no correction be made for cloud amounts less than 0.25 of total sky was

followed. Sea surface albedo, α, was extracted from Payne's (1972) tables, following Nelson and Husby's (1983) algorithm which involves entering the tables with the 0.7 atmospheric transmission coefficient, reduced by a factor equal to the cloud correction applied in Equation (3), and with the mean daily solar altitude.